

EXPERIMENTAL INVESTIGATION OF THE FREE SURFACE EFFECT ON THE CONICAL TAYLOR-COUPETTE FLOW SYSTEM

F. Yahi^{1,2}, Y. Hamnoute¹, S. Lecheheb¹ and A. Bouabdallah¹

¹Thermodynamics and Energetic Systems Laboratory, Faculty of Physics. University of Sciences and Technology Houari Boumediene, B.P.32 El Alia 16111 Bab Ezzouar. Algiers, Algeria.

²Departement of hydrocarbons transport, University M'Hamed Bougara–35000 Boumerdes-Algeria

Abstract

The aim of this work is to highlight the critical thresholds corresponding to the onset of different instabilities considered in the flow between two vertical coaxial cones with and without free surface. The inner cone is rotating and the outer one is maintained at rest. Both cones have the same apex angle $\Phi = 12$ giving a constant annular gap $\delta = d/R_{1\max}$. The height of the fluid column is $H = 155\text{mm}$ and can be progressively decreased for each studied case of the flow system. Two kinds of configuration are studied, small and large gap configurations. The working fluid is assumed as Newtonian and having constant properties as density and viscosity within the range of the required experimental conditions. By means of visualization technique of the flow we were able to show the different transition modes occurring in the conical flow system according to the aspect ratio and then the induced action of the free surface which introduces a delay in the onset of different instability modes. The obtained results in term of features and stability of the flow are compared to those of M. Wimmer [3-8] and N Noui-Mehidi [9].

Keywords: conical Taylor-Couette flow, free surface effect, transition

1 Introduction

The flow between rotating coaxial cylinders has been the subject of numerous theoretical and experimental works [1-2]. G.I. Taylor (1923) [1] was the first author who predicted the onset of the first instability: axial stationary wave consists of two contra-rotating vortices. Thereafter this kind of rotational motion has been generalized to various geometries such as flow between coaxial spheres [3-6] and between coaxial cones [3]. As well as in industrial processes, this flow system is has a great importance, not only in the design of rotating machinery such as multiple concentric drives, turbine rotor, but also for the application to chemical equipment such as compact rotating heat exchangers and mixers.

The flow between rotating cones has been studied experimentally and numerically by several authors. M. Wimmer [3] has studied Taylor-Couette flow in different geometries: cylindrical, spherical, conical and between coaxial ellipsoids and has investigated the combination between cone and cylinder. M.N. Noui Mehidi et al [7] have examined the laminar-turbulent transition in the case of small gap configuration and showed that the flow develops from the laminar regime towards helical motion through the formation of Taylor vortices by varying the rotation speed of the inner cone. In 1995, M. Wimmer [8] investigated the appearance of Taylor vortices in different gap configurations, with the inner rotating and the outer at rest, and found that the flow is three dimensional. M.N. Noui Mehidi and M. Wimmer [9] studied the flow states occurring in the presence of free surface in the case of large gap configuration.

In this work, we consider the conical flow with small and large gap configurations. Our primary interests are to carry out a systematic experimental study, focusing on analysis of laminar-turbulent regime to highlight the transition process from order to disorder including the appearance of different instability modes to triggering the chaos. In the Light of the work of M. N. Noui Mehidi and M. Wimmer [9] as well as work of A. Mahamdia [10-11] devoted to the effect of free surface on Taylor-Couette flow, we are motivated to perform this study which will

allow us to highlight the influence of the free surface on viscous fluid flow between two coaxial cones whose inner cone is rotating and the outer one is at rest. Two kinds of configuration are investigated, large and small gap in order to highlight the effect of the free surface that has been studied only in the wide gap configuration ($\delta = 0.25$). The main purpose of our study is to derive a comparison between the present case (small gap) and the nominal case existed in the specialized literature (large gap). The effect of free surface on the onset of different instability modes, cells number, axial wavelenght and axial velocity is systematically examined. The obtained results are compared with those of M. Wimmer and M. N. Noui Mehidi in the case of large gap configuration.

2 Experimental devices

The experimental device consists of two coaxial cones made of insulating and transparent material (Plexiglas) in order to allow a good visualization of flow regime. Both cones have the same apex angle $\Phi = 12^\circ$ giving a constant annular gap $\delta = d/R_{1max}$ that $d = (R_{2max} - R_{1max})$. The inner cone is rotated and the outer one is maintained at rest.

Two kinds of configuration have been investigated: a small annular gap configuration $d_1 = 4.85$ mm and large annular gap $d_2 = 9.68$ mm. Our system is characterized by an outer cone with larger radius $R_{2max} = 45$ mm and lower radius $R_{2min} = 12$ mm. The length of the fluid column is fixed at $H = 155$ mm. The larger radius of the inner cone R_{1max} varies between 40.15 mm and 35.31 mm, while the lower radius R_{1min} ranges from 7.15 mm and 2.32 mm. The inner cone is driven by a DC motor connected to the rotating axis by a flexible tube in order to avoid the adverse effects of vibration, (Figure 1).

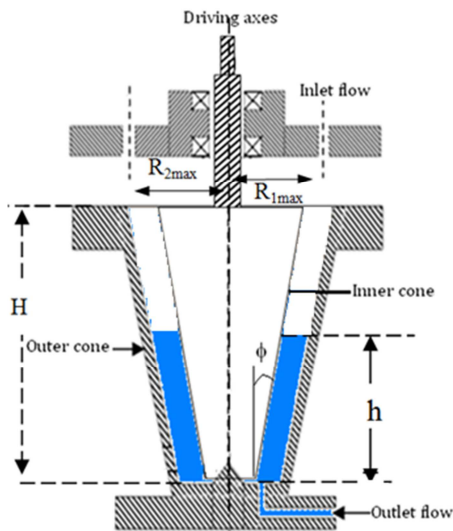


Figure 1: Conical Taylor-Couette flow system

Geometric		Dynamic
Radial gap $\delta = d/R_{1max}$	$\delta_1 = 0.12$ (small gap)	Reynolds number $Re = R_{1max} \Omega d / \nu$
	$\delta_2 = 0.27$ (large gap)	Taylor number $Ta = (R_{1max} \Omega d / \nu) \delta^{1/2}$
Aspect ratio $\Gamma = h/d$ (axial limitation)	$9.6 < \Gamma_1 < 32$ $3.1 < \Gamma_2 < 16$	Froude number $Fr = R_{1max} \Omega / \sqrt{gh \cos \phi}$

Table 1: Control parameters

The display product used is a solution of 20% of Vaseline oil CHALLALA, favoring a better suspension of the particles in the fluid visualization, which is added to 80% of a petroleum product SIMILI to reduce the viscosity of the oil in a concentration of 2g/l of aluminum flakes. Such that the mixture constitutes a Newtonian fluid characterized by kinematic viscosity $\nu = 4.8 \cdot 10^{-6} \text{ Cm}^2/\text{s}$ and a density $\rho = 777.23 \text{ kg/m}^3$.

In order to characterize the onset of hydrodynamic instabilities, it is necessary to introduce dimensionless numbers involving viscous forces that play a stabilizing role and centrifugal forces which have a destabilizing role. The manifestation of a given waveform or instability was

identified using the control parameters of flow namely the Reynolds number Re , the Taylor number Ta and the Froude number Fr defined in the Table 1.

Three visualization techniques have been used:

Reflection of natural light: This method is based on light beam reflecting from seeding particles. The light is supplied by external source situated in front of the experimental device, in order to highlight the nature and the properties associated with the flow structure. The mechanism of this technique is about properties of reflected light depending on the orientation of the velocity vector. If it is axial, the particles reflect light completely and the present gives us the maximum velocity of the cell. On the contrary, if the velocity has a significant radial component, the particles will be oriented parallel to the light rays and let the light pass without reflection; in this case the velocity is minimal (Figure 2).

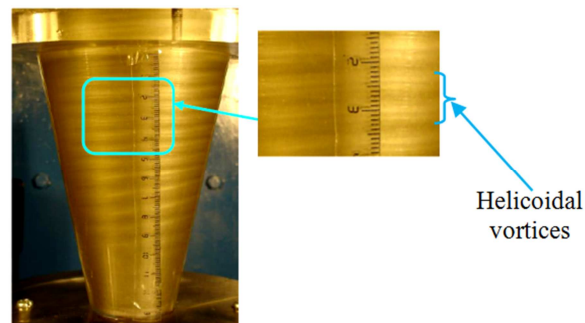


Figure 2: Natural light reflection $\delta_1 = 0.12$, $\Gamma = 32$ $Ta = 64.9$

Transmission of natural light: This method of visualization is based on the optical transmission of the light source which is placed behind the experimental device. The light rays pass through the flow and provide picture of the flow structure (Figure 3).

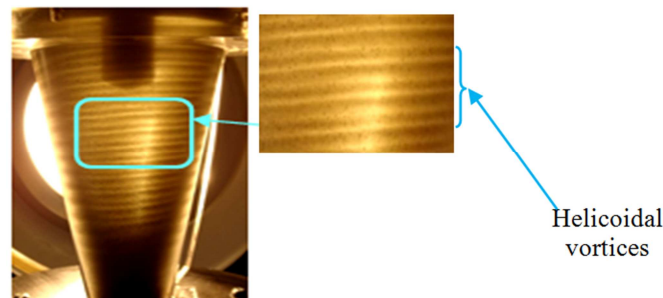


Figure 3: Natural light transmission $\delta_1 = 0.12$, $\Gamma = 32$ $Ta = 72$

Laser transmission is used to give more information on the local flow structure (Figure 4).

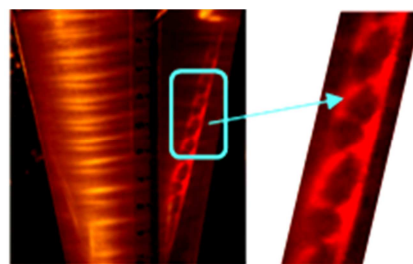


Figure 4: Laser transmission visualization $\delta_1 = 0.12$, $\Gamma = 25.8$ et $Ta = 88.5$

3 Results and Discussions

For both configurations small $\delta_1 = 0.12$ and large annular gap $\delta_2 = 0.27$ and for a given aspect ratio Γ in the interval $9.6 < \Gamma_1 < 32$ and $3.1 < \Gamma_2 < 16$, we investigate the basic flow and the laminar-turbulent transition regime.

3.1 Basic flow

The basic flow is laminar three-dimensional for $Ta < Tc_1$ in the whole range of aspect ratio Γ . It results from the imbalance between the viscous and centrifugal forces that exist in the absence of any disturbance. The three-dimensional nature of the flow is mainly due to the linear variation of the centrifugal forces caused by the linear variation of the radius versus the conical axial position "z". The flow is a homogeneous movement throughout the fluid column, characterized by a perfect symmetry in the axial and azimuthal directions.

3.2 Transition regimes

3.2.1 Completely filled system

For a completely filled system the fluid is limited by end plates, where the non-slip condition applies and causes a deceleration of the fluid. For a constant radial gap and with increasing the angular velocity of the inner cone, the centrifugal forces will progressively dominate the viscous forces. Disturbances of the basic flow then generate regular closed vortex cells. The first cell of Taylor appears in the vicinity of the upper edge where the centrifugal forces are largest. This toroidal cell is stationary; its size is of the order of the annular gap and forms a pair of cells with the rest of the flow. The Taylor number value corresponding to the appearance of the Taylor vortex (TV) is $Ta = Tc_1$. By increasing gradually the inner cone velocity we observe the appearance of a second cell that propagates along the downward helical motion characterized by the Taylor number $Ta = Tc^{DHM}$. The principal cause of this downward movement of the vortex is the rotation of the cell around on itself and when the mass transport is compensated in such a helical vortex tube. Near $Ta = Tc_1$ we note the formation of two different flow zones: one evolving in a supercritical flow regime (unstable laminar flow) and the other is governed by a subcritical flow regime (laminar stable) Figure 5. The azimuthal wave or "Wavy Mode" appears in the upper part of the annulus with very low amplitude corresponding to the critical Taylor number $Ta = Tc_2$, then the other part of the cells preserves the same properties as those described above. The existence of this second instability gives rise to a doubly periodic flow which propagates in the axial and azimuthal directions. For $Ta = Tc^{UHM}$ we note the superposition of three flow instabilities, namely, downward helical motion, upward helical motion and wavy mode.

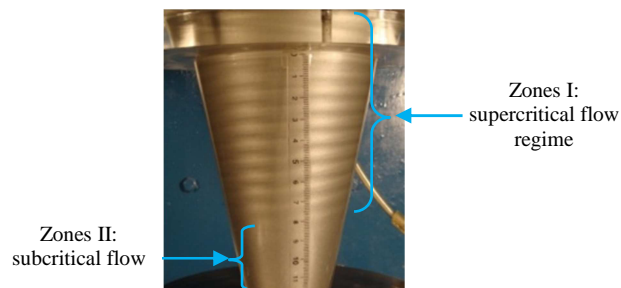


Figure 5: Visualization of sub and supercritical regime $Ta = 61.1$, $\Gamma = 32$ (DHM)

By observing Table 2 we can see that the obtained results are in good agreement with those of M.Wimmer [3, 8, 16 and 17] in the case of a small annular gap. The Taylor number value corresponding to the onset of the Taylor vortices in the case $\delta_1 = 0.12$ is close to that obtained by M.Wimmer [3, 8, 16 and 17] for a radial gap $\delta = 0.11$. It is also very close to that obtained in

the cylindrical geometry near to 2.4% for small gap configuration, whereas the discrepancy was 5.6% for the downward helical motion. This value coincides with that obtained in spherical geometry $T_s = 57.62$ evaluated at 3.2% in the case $\delta = 0.14$ [5]. In addition, the discrepancy corresponding to the appearance of the azimuthal wave is 7.7% compared with the work of M.Wimmer [8, 16 and 17].

Table 2. Comparison of critical Taylor number values for different gap configurations
(completely filled flow system)

Critical Taylor Number		T_{c1}	$T_{c,DHM}$	T_{c2}	$T_{c,UHM}$
Flow Regimes		Taylor Vortices Flow TVF	Down helical Motion DHM	Wavy Vortices Flow WVF	Upward helical Motion UHM
M.Wimmer [3, 8, 16 and 17]	$\delta = 0.11$	41.6	50	74.9	
Presentwork	$\delta_1 = 0.12$	42.3 1.7%	47.2 5.6%	68.8 7.65%	72
M.Wimmer [3, 8, 16 and 17]	$\delta = 0.25$	46.7	57	68	-
Present work	$\delta_2 = 0.27$	65.8 41.5%	85.1 25%	145.6	189.3

In the case of a large gap configuration $\delta_2 = 0.27$, it was found that the relative discrepancy in the Taylor number value corresponding to the onset of the (TV) becomes very large 41.5%; while one corresponding to the establishment of the downward helical motion is about 25% because when the annular spaces becomes larger, the instabilities installation becomes slower and introduces an onset delay.

Some flow states for the small gap configuration corresponding to $\delta_1 = 0.12$ are shown in Figure 6.

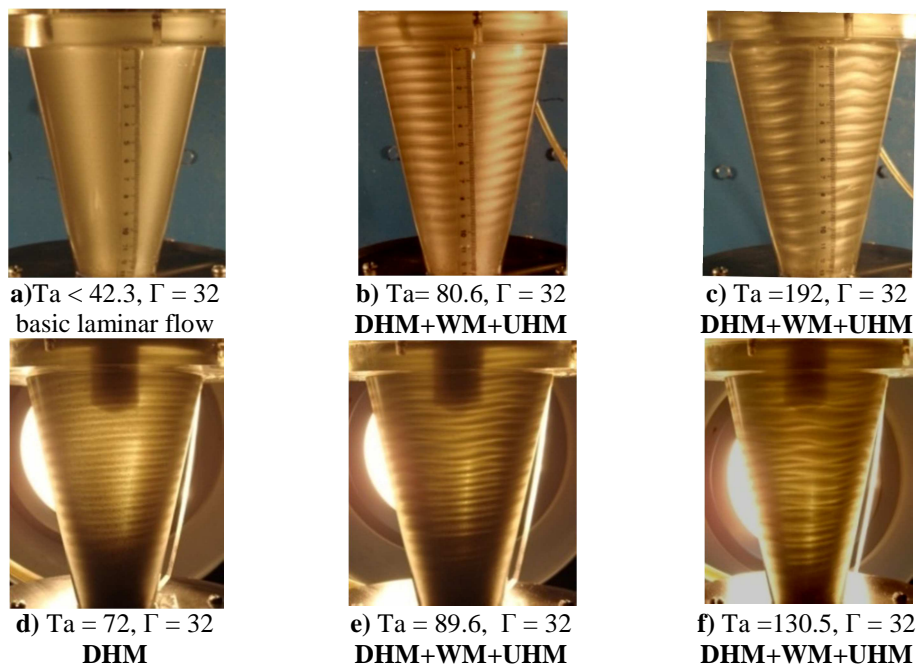


Figure 6: Flow visualization states: a), b) and c) Natural light reflection. d), e) and f) Natural light transmission $\delta_1 = 0.12$

3.2.2 Partially filled system

In presence of free surface a strong deceleration cannot take place, so that the angular velocity in the vicinity of free surface is higher than at a stationary end plate. The higher velocity leads to highest centrifugal forces resulting in the appearance of instabilities.

For the partially filled flow system $\Gamma < 32$, the existence of a vortex ring induced by the free surface is observed before the onset of the Taylor vortex. This so-called free surface cell undergoes torsion during the appearance of the first steady cell which is settled in the vicinity of the free surface (Figure 7).

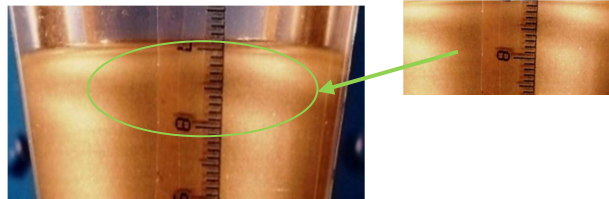


Figure 7: Warping phenomenon visualization

The analysis of this vortex has allowed determining the evolution of its size "e" in function of filling ratio, as well as its angle θ relative to the horizontal axis. The size of this vortex is higher for low aspect ratio $9.6 \leq \Gamma \leq 17.5$ ($e = 9\text{mm}$). Then it tends to decrease to a value of 0 for $\Gamma = 32$ according to a polynomial law. However, the angle θ follows an exponential growth (Figure 8).

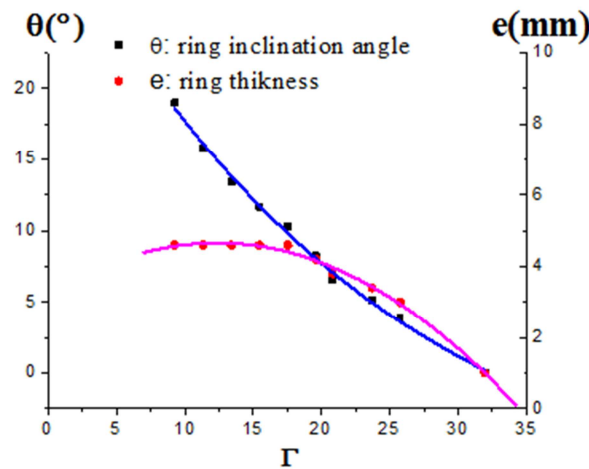


Figure 8: Evolution of the thickness and the inclination angle of the ring in the vicinity of the free surface

For small gap configuration $\delta_1 = 0.12$ and different filling ratio values $9.6 \leq \Gamma < 32$, the first cell is inclined in the opposite direction of the free surface vortex and is delayed at onset of 11% to 66% compared to the completely filled flow system. Whereas for relatively large configuration $\delta_2 = 0.27$ this delay is very important and is between 55% and 200%. The Taylor number corresponding to the first instability, changes according to a linear law with negative slope of (-1.1), whereas, the Froude number evolves according to a polynomial law with aspect ratio Γ in the range $9.6 \leq \Gamma < 32$ in the case of the small gap configuration $\delta_1 = 0.12$.

Azimuthal wave is delayed by 16% to 60%, up to a critical height $\Gamma_c = 15.5$. At this threshold it disappears Figure 9 (a). This delay is produced by the free surface and is mainly due to the meridional component velocity of the flow.

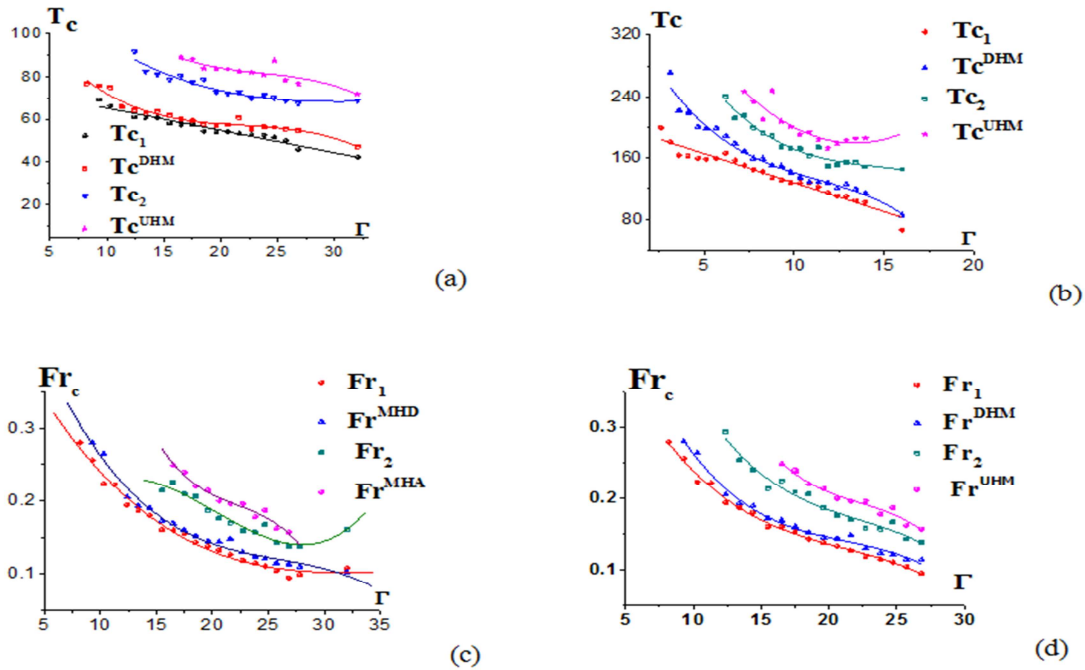


Figure 9: Evolution of the number critical Taylor (**a, b**) and the critical Froude number (**c, d**) depending on the filling rate Γ for both configurations

Conclusion

The study of the transition to turbulence in the conical Taylor–Couette flow system is motivated in part by hope that general modes of transition can be developed. The present experiments indicate that chaotic regime occurs after a small number of transitions to distinct modes: Taylor vortices mode, downward helical motion, wavy mode and upward helical motion in the small and large configurations. In the case of completely filled flow system there is a direct transition to chaos while the flow system is partially filled there are some modifications preceding turbulence.

For $\Gamma < 32$, a vortex ring induced by the free surface is observed before the onset of the Taylor vortex. This so-called free surface cell undergoes torsion during the appearance of the first steady cell which is settled in the vicinity of the free surface.

The axial limitation of the flow introduces a considerable delay in the appearance of the first instability (Taylor vortices), the onset of spiral wave and azimuthal wave as well. In particular, we observe the disappearance of the azimuthal wave for a critical value of aspect ratio $\Gamma = \Gamma_{c1} = 15.5$ ($\delta_1 = 0.12$) and $\Gamma = \Gamma_{c2} = 6.7$ ($\delta_2 = 0.27$).

The major interest in these experiments in both cases of flow system configurations is the properties of the free surface, such as the interaction on the mode formations, its characteristics: axial wavelength, axial velocity and globally a stabilizing effect of the whole movement in the conical Taylor-Couette flow system.

The research reported here will be continued with experiments by spectral analysis on selective Γ as Taylor number Ta increases to determine the evolution of mode formations in laminar-turbulent transition regime.

References

- [1] G. I Taylor: Stability of a viscous liquid contained between two rotating cylinders, *Phil. Trans. R.Soc. London Ser. A* 223, 289-343 (1923).

-
- [2] Kádár R., Balan C.: Transient dynamics of the wavy regime in Taylor–Couette geometry, *Eur. J. M. B/Fluids* 31158-167 (2012).
- [3] Wimmer M.: Viscous flows and instabilities near rotating bodies, *Prog. Aerospace Sci.* 25, 43-103 (1988).
- [4] Wimmer M.: Experiments on a viscous fluid flow between concentric rotating spheres, *Journal of Fluid Mechanics* 78, 317-335 (1976).
- [5] Sha W. et Nakabayashi K.: On the structure and formation of spiral Taylor-Gortler vortices in spherical Couette flow, *Journal of Fluid Mechanics*, 295, 43-60 (2001).
- [6] Nakabayashi K.: Characteristics of disturbances in the laminar–turbulent transition of spherical Couette flow. *Phys. Fluids* 14, 39-63 (2003).
- [7] Noui - Mehidi M. N. et Bouabdallah A.: A laminar-turbulent transition in the flow between rotating coaxial cones, *Proc. 3rd Int. Workshop on electro-diffusion diagnostics of flow*, CNRS 139-147 (1993).
- [8] Wimmer M.: An experimental investigation of Taylor vortex flow between conical cylinders, *Journal of Fluid Mechanics* 292, 205-227 (1995).
- [9] Noui-Mehidi M.N. and Wimmer M.: Free surface effects on the flow between conical cylinders, *Acta Mechanica* 135, 13-25 (1999).
- [10] Mahamdia, A. et Bouabdallah A.: Effets de la surface libre et du rapport d'aspect sur la transition de l'écoulement de Taylor- Couette, *CRAS -Paris Mécanique*, Vol 331, N°3, 245-252, (2003).
- [11] Bouabdallah A.: Instabilités et Turbulence dans l'écoulement de Taylor-Couette, *Thèse de Doctorat ès Sciences, INP Lorraine*, (1980).
- [12] Noui -Mehidi M.N., Ohmura N. and Kataoka K.: Flow modes selection and transition in conical cylinders system *12th I. C.T.W, September* 6-8 (2001).
- [13] Noui-Mehidi, M.N., Ohmura, N., Kataoka, K.: Mechanism of mode selection for Taylor vortex flow between coaxial conical rotating cylinders. *Journal of Fluids and Structures* 16, 247–262 (2002).
- [14] Noui-Mehidi M .N. et al: Dynamics of the helical flow between rotating conical cylinders *Journal of Fluids and Structures* 20,331-334 (2005).
- [15] Ohmura N., Noui Mehidi M.N. et al: Mixing characteristics in a conical Taylor-Couette Flow System at Low Reynolds numbers, *J.Che. Eng. of Japan.* 37, 546-550 (2004).
- [16] Wimmer M. and Zierep J.: Transition from Taylor vortices to cross-flow instabilities, *Acta Mechanica* 140, 17-30 (2000).
- [17] Wimmer M.: Taylor vortices at different geometries. *In: Egbers, C., Pfister, G. (Eds.), Physics of Rotating Fluids. Springer, Berlin*, pp. 195–212 (2000).